Asociación Argentina
de Mecánica Computacional

Mecánica Computacional Vol XXVII, págs. 159-168 (artículo completo)
Alberto Cardona, Mario Storti, Carlos Zuppa. (Eds.)
San Luis, Argentina, 10-13 Noviembre 2008

NUMERICAL STUDY THROUGH FINITE DIFFERENCES OF THE ILL-POSED INITIAL CONDITIONS IN THE CLASSICAL MELT SPINNING MODEL

Mariel L. Ottone, Marta B. Peirotti and Julio A. Deiber

Instituto de Desarrollo Tecnológico para la Industria Química
(INTEC-UNL-CONICET)
Güemes 3450, S3000GLN, Santa Fe, Argentina
e-mail: treoflu@ceride.gov.ar

Key words: Spinning Flow, Finite Differences, Initial Conditions, Elongational Flow

Abstract. The non isothermal melt spinning process at low take up velocities is composed of three distinctive zones of major interest for research. One is associated with the 1-D flow in the extrusion capillary. The second one starting at the capillary end is designated swelling zone, and presents a 2-D flow where the filament relaxes before entering the 2-D spinning flow (the third zone). Here, elongational deformations predominate before the solidified filament is taken at the spinneret end. The purpose of the present work is to analyze numerically within the structure of the classical melt spinning model the relevance of the unknown axial position after the swelling zone, where initial conditions of the non isothermal spinning flow are imposed. This aspect constitutes an ill-posed problem that must be analyzed carefully in relation to the useful numerical results obtained along the spinning length relatively far from the swelling zone. In this context of analysis, our results provide a new insight of this problem and also show that an additional physical constraint may lead one to place appropriate initial conditions for computational purposes. This constraint is based on the consideration of the rheometric and process elongational viscosity curves. The Phan-Thien and Tanner viscoelastic constitutive equation is used here to illustrate main results and conclusions of the present work.

1 INTRODUCTION

The classical non-isothermal melt spinning flow at low take up velocities is modeled in the literature by considering a filament of polymer melt that is continuously drawn and simultaneously cooled with air. This process finally yields a solidified yarn. All the filaments of the spinneret are assumed to achieve, in principle, the same properties during the spinning process, and they compose the synthetic fiber in a bobbin. For these purposes a model describing the velocity, stress and temperature fields in one filament may be useful to control the quality of the final product (Denn, 1980). More recently, we provided a computational algorithm based on finite differences to obtain the axial velocity profile and the thermal and stress fields in the 2-D domain of the filament (Ottone and Deiber, 2002). In this work, the perturbation analysis of the full spinning model reported by Henson et al., (1998) was considered. This model was formulated for the low speed range (flow induced crystallization was not considered) through a regular perturbation analysis that included the slenderness approximation associated with long fibers of very small diameters. From previous works, it is clear that the radial and axial stress and temperature fields in the melt fiber spinning process may be estimated within a consistent theoretical framework. Also, we have available a robust numerical algorithm computing the resulting momentum and energy balances coupled to typical viscoelastic constitutive equations.

Therefore, the purpose of the present work is to analyze numerically within the structure of the perturbed 2-D model mentioned above, the relevance of the unknown axial position around the swelling, where initial conditions of the classical model (initial velocity, stresses and temperature) are imposed. This aspect constitutes an ill-posed problem that must be analyzed carefully in relation to the useful numerical results obtained along the spinning length relatively far from the swelling zone. It is also necessary to discuss in detail, how the types (instantaneous or retarded responses) of constitutive models affect numerical procedures and results, in order to choose the appropriate axial position for initial conditions. For this task, our iterative numerical algorithm is used, and results are obtained for a typical take up velocity (3000 m/min). The discrete non-isothermal melt spinning model is expressed in finite differences, which involve the implicit tri-diagonal algorithm for the temperature field, and explicit-implicit backward differences for the stresses. Fine meshes can be generated to obtain the required precision. Therefore, in this context of analysis, our results provide a new insight of this ill-posed problem involving non-isothermal melt spinning flows, and also show that an additional physical constraint may lead one to appropriate initial conditions. This constraint is based on the consideration of the rheometric and process elongational viscosity curves, defined below. Here the Phan-Thien and Tanner viscoelastic constitutive equation, which is appropriate to describe extensional flows, is used to illustrate our conclusions. The study is carried out for polyethylene terephthalate (PET), which is a typical synthetic polymer used in the commercial production of fibers.

2 CLASSICAL MELT SPINNING MODEL

The melt spinning model considered here was formulated in the steady state regime by Ottone and Deiber (2002). Therefore, in this section, we present a brief description of this model in order to carry out then the study concerning the ill-posed nature of the initial conditions invoked above. Thus, the polymer is considered incompressible and hence the mass balance implies,

$$\left(\underline{\nabla} \cdot \underline{v}\right) = 0 \tag{1}$$

where $\underline{v}$ is the velocity vector. Also the momentum balance in the filament is expressed,

$$\rho \underline{v} \cdot \underline{\nabla v} = -\underline{\nabla} p + \underline{\nabla} \cdot \underline{\underline{\tau}} + \rho \underline{g} \tag{2}$$

In Eq. (2), ρ is the polymer density, p is the pressure field, $\underline{g}$ is the gravity vector and $\underline{\underline{\tau}}$ is the extra stress tensor. The energy balance in the filament is,

$$\rho c_v \underline{v} \cdot \underline{\nabla} T = -\underline{\nabla} \cdot \underline{q} + \underline{\underline{D}} : \underline{\underline{\tau}} \tag{3}$$

where $c_v = a + bT$ is the polymer thermal capacity, a and b are thermo-physical constants and T is the temperature field. In addition $\underline{q} = -k_s \cdot \underline{\nabla} T$ is the heat flux vector, where k_s is the thermal conductivity, and $\underline{\underline{D}} : \underline{\underline{\tau}}$ is the mechanical power. In this term the rate of deformation tensor $\underline{\underline{D}} = (\underline{\nabla v} + \underline{\nabla v}^T)/2$ is a function of the fluid kinematics $\underline{v}(r,z) = v_z \underline{e}_z + v_r \underline{e}_r$, where v_z and v_r are the axial and radial components of the velocity vector, respectively, in the cylindrical coordinate system.

Boundary conditions to solve Eqs. (1) to (3) are the same as those reported by Ottone and Deiber (2002). Here the Phan-Thien and Tanner viscoelastic model (PTTM), which is appropriate to describe extensional flows, is used (see below). This model includes the retarded elastic response $\underline{\underline{\tau}}_s = 2\eta_s \underline{\underline{D}}$ and hence initial values for τ_s^{zz} and τ_s^{rr} are needed at z=0, apart from the stress ${\tau_p}^{zz}$ and the relation $R = {\tau_p}^{rr} / {\tau_p}^{zz}$ already discussed in the literature (Denn, 1983). This requirement is equivalent to assign a value to the axial velocity derivative at $z = 0$. Thus the additional initial condition needed and expressed $f = \partial v_z / \partial z$ is basically an ill-posed problem in the spinning literature because its specific value is unknown. It must be determined with a physical criterion (for instance, the null velocity derivative at the maximum filament swelling may be a choice). In fact, it was found with the PTTM that when $f \to 0$, numerical solutions obtained for the average temperature and axial velocity of the filament, far from the initial position, were not dependent on the different small values assigned to this derivative (Ottone and Deiber, 2002). On the other hand, when the rheological model with instantaneous elastic response was used (the term $\underline{\underline{\tau}}_s$ was not included) the condition $f \approx 0$ is not satisfied for any assumed initial filament radius, and hence, the position $z = 0$ is not well determined in relation to the capillary exit. Usually, in this case authors suggest placing it around two to four capillary diameters below the capillary exit (Keunings et al., 1983).

In the sense discussed above, the origin of the coordinate system may be placed either at the maximum swelling of the polymer melt or at a higher distance depending on the value $f = 0$ or $f > 0$, respectively, where the filament enters a monotonic stretching flow at given distance from the exit of the extrusion capillary. At the position of the initial conditions, where $z = 0$, the mechanical and thermal fields are assumed uniform in the radial direction. Therefore throughout this work the initial conditions (essentially the spatial-initial conditions) for any value r are,

$$v_z = v_s, \qquad T = T_o$$

$$r_o(0) = r_s, \qquad \tau^{zz} = \tau_o^{zz}, \qquad R = \frac{\tau^{rr}}{\tau^{zz}} \tag{4}$$

In Eq. (4), $r_o(z)$ is the fiber radius as a function of the axial direction z, v_s is the melt velocity at the onset of the spinning flow with radius r_s, and T_o is the extrusion melt

temperature. Thus, $v_s = v_c r_c^2 / r_s^2$ where v_c is the melt averaged velocity in the extrusion capillary of radius r_c. It has been discussed in the literature that the condition $R \approx 0$ is a good approximation (Denn, 1983; Gagon and Denn, 1981; Denn et al., 1975). At the end of the spinneret ($z = z_L = L$) the take up velocity is $v_z = v_L$; hence the drawratio is $DR = v_L / v_s$.

The symmetry of mechanical and thermal fields is imposed at the centerline $r = 0$ for any position *z*. Thus,

$$\frac{\partial v_z}{\partial r} = 0\,, \quad \frac{\partial T}{\partial r} = 0\,, \quad \frac{\partial \tau^{zz}}{\partial r} = 0, \quad \frac{\partial \tau^{rr}}{\partial r} = 0 \tag{5}$$

In addition at the filament free surface for $r = r_o(z)$ and any position *z*, dynamics and kinematics constraints are,

$$\left(\underline{\underline{T}} \cdot \underline{n}\right) \cdot \underline{t} = \left(\underline{\underline{T}}_a \cdot \underline{n}\right) \cdot \underline{t} \tag{6}$$

$$\left(\underline{\underline{T}} \cdot \underline{n}\right) \cdot \underline{n} = -\sigma \aleph + \left(\underline{\underline{T}}_a \cdot \underline{n}\right) \cdot \underline{n} \tag{7}$$

$$\underline{v} \cdot \underline{n} = 0 \tag{8}$$

$$\underline{v} \cdot \underline{t} = \underline{v}_a \cdot \underline{t} \tag{9}$$

for the mechanical variables and,

$$\underline{q} \cdot \underline{n} = h_e \Delta T \tag{10}$$

for the temperature field. In these equations, $\underline{n}$ and $\underline{t}$ are the unit vectors normal and tangential to the free surface, respectively. $\aleph$ is the curvature of the free surface and σ is the polymer-air surface tension. In addition, the stress tensor $\underline{\underline{T}} = -p\underline{\underline{\delta}} + \underline{\underline{\tau}}$ involves the extra stress tensor $\underline{\underline{\tau}}$ and the pressure *p*, where $\underline{\underline{\delta}}$ is the unit tensor. In Eq. (10), $\Delta T = T - T_a$ is the thermal jump between the average air temperature T_a used to cool the fiber and the polymer temperature *T* evaluated at the free surface. Also the external coefficient of heat transfer h_e may be evaluated through correlations reported by Denn (1996). We designate *L* the length from the initial condition to the position where the melt reaches the glassy temperature T_g to become solidified. In Eqs. (6) to (8), $\underline{\underline{T}}_a$ is the stress tensor and $\underline{v}_a$ is the velocity vector, both of the cooling air (see Ottone and Deiber, 2002, for more details).

To complete the formulation of the spinning model, the viscoelastic stress $\underline{\underline{\tau}}_p$ is required, which is a part of the total extra stress tensor $\underline{\underline{\tau}} = \underline{\underline{\tau}}_p + \underline{\underline{\tau}}_s$, where $\underline{\underline{\tau}}_s$ is associated with retardation effects, as indicated above. In this sense, the PTTM is expressed,

$$\underline{\underline{\tau}}_p + \lambda \frac{\delta}{\delta t} \underline{\underline{\tau}}_p = 2\lambda G \underline{\underline{D}} \tag{11}$$

where,

$$\frac{\delta}{\delta t} \underline{\underline{\tau}}_p = \frac{D}{Dt} \underline{\underline{\tau}}_p - \underline{\underline{L}} \cdot \underline{\underline{\tau}}_p - \underline{\underline{\tau}}_p \cdot \underline{\underline{L}}^T - \underline{\underline{\tau}}_p \frac{D \ln T}{Dt} \tag{12}$$

is the non-affine convective time derivative; here the effect of the thermal history is added through the term $D\ln T/Dt$. Also $\underline{\underline{L}} = \underline{\underline{\nabla v}} - \chi \underline{\underline{D}}$ is the effective velocity gradient tensor and $\eta_s = \eta_p(1-\alpha)/\alpha$ with $\eta_p = \lambda G$. Therefore, the instantaneous elastic response of the PTTM is obtained for $\alpha = 1$.

Since rheological models get the linear viscoelastic response at the asymptotic limit of small shear rates, the basic relaxation time λ_o is expressed $\lambda_o = 0.016\, exp\{-11.9755 + 6802/(T+273)\}$ as reported by Gregory and Watson (1970). In particular, the PTTM considers an effective relaxation time that is a function of the stress tensor expressed $\lambda = \lambda_o(T)/K(T, tr\underline{\underline{\tau}})$ where $K = exp(\xi\, tr\underline{\underline{\tau}}/G)$. In this context of analysis the relaxation modulus is also allowed to change with temperature according to $G = G_o(T/T_r)$ where T_r is the reference temperature.

Rheometric characterizations of the PTTM were carried out by following the same procedure described by Ottone and Deiber (2000) to evaluate the rheological parameters of the PET melt with experimental data reported by Gregory and Watson (1970) involving the shear rate flow of a sample that had the same intrinsic viscosity as the PET used by George (1982) (zero shear rate viscosity $\eta_o \approx$ 104.9 Pa s). The results obtained are $\alpha \approx 0.85$, $\chi \approx 4\ 10^{-5}$ and $\xi \approx 9.25\ 10^{-5}$.

To facilitate the discussion of results in Section 4, throughout this work the extensional viscosity is expressed,

$$\eta_e(T, \dot{\varepsilon}) = \frac{\left(\tau^{zz} - \tau^{rr}\right)}{\dot{\varepsilon}} \tag{13}$$

where $\dot{\varepsilon} = (\partial v_z / \partial z)$ is constant under rheometric conditions. In a similar framework, the process extensional viscosity is defined as follows,

$$\eta_e{}^p\left(T, \dot{\varepsilon}^p\right) = \frac{\left(\tau^{zz} - \tau^{rr}\right)^p}{\dot{\varepsilon}^p} \tag{14}$$

where the process extensional rate is obtained from $\dot{\varepsilon}^p = (\partial v_z / \partial z)^p$ by using the spinning axial velocity. Once the interplay between process and extensional rheometric variables has been defined, master curves of both viscosities are carried out by using the thermal shift factor a_T, expressed,

$$a_T = \frac{\lambda_o(T)}{\lambda_o(T_r)} = \frac{\lambda_o(T)}{\lambda_{oo}} = \exp\{-11.9755 + \frac{6802.1}{(T+273)}\} \tag{15}$$

for the PET under consideration.

3 FRAMEWORK OF THE NUMERICAL METHOD

The numerical method solving the model equations (Eqs.(1) to (15)) has been described in detail in Ottone and Deiber (2002). Basically, we use the regular perturbation scheme proposed by Henson et al. (1998) to obtain the perturbed 2-D model. This scheme allows one to neglect rigorously terms of small orders from the balance and constitutive equations and the boundary conditions of the complete model. Then the perturbed 2-D model is averaged in the radial direction of the filament, without any approximation, to yield an appropriate version of the perturbed average model.

It is relevant to indicate that the complete model described by Eqs (1) to (15) is quite difficult to solve due to the presence of the free interface, the highly non linear terms in the constitutive equation as well as to the ill-pose nature of the initial condition after the extrusion capillary. The perturbed model obtained is able to preserve the most relevant physical phenomena of the non isothermal spinning.

The perturbation analysis is carried out on the complete model by expressing any dependent variable, designated P in the generalized sense, through the series $P = \sum_{n=0}^{\infty} \Lambda^n P^{(n)} = P^{(o)} + \vartheta(\Lambda)$. Here Λ is the ratio between the capillary radius and the stretching length of the filament. Then, terms of order Λ and greater orders are neglected to introduce the slenderness hypothesis. The result is the "perturbed 2-D model". In this framework, a coordinate transformation is introduced to consider the axial variation of the filament radius $r_o(z)$. Thus, new coordinates $Z = z$ and $\zeta = r/r_o(z) = r/r_o(Z)$ are defined to obtain a rectangular computational domain (Deiber and Schowalter, 1979). As indicated above, the numerical algorithm proposed in this work requires a rigorous averaging in the radial direction of the perturbed equations. This radial average is defined as follows,

$$\langle P \rangle = 2\int_0^1 P(Z,\zeta)\,\zeta\, d\zeta \tag{16}$$

to obtain a set of equations that conforms the "perturbed average model". Consequently the basic strategy of the numerical algorithm is to solve the coupled perturbed 2-D and average models through an iteration process. In order to compute simultaneously these models, they are written in finite differences. Therefore the perturbed averaged model can be expressed in the matrix form $\dot{\underline{x}} = \underline{\underline{A}}^{-1}(\underline{x}) \cdot \underline{b}$ where $\dot{\underline{x}} = \{\frac{\partial v_z}{\partial Z}, \frac{\partial f}{\partial Z}, \frac{\partial < \tau_p^{zz} >}{\partial Z}, \frac{\partial < \tau_p^{rr} >}{\partial Z}, \frac{\partial < T >}{\partial Z}\}$ and $f = \partial v_z / \partial Z$ (see Ottone and Deiber, 2002). It is clear that these equations require the stress fields $\tau^{zz}(Z,\zeta)$ and $\tau^{rr}(Z,\zeta)$ and the temperature field $T(Z,\zeta)$ to evaluate the non-linear averages indicated with $< \cdot >$ and involved in the matrix $\underline{\underline{A}}^{-1}(\underline{x})$. Equation $\dot{\underline{x}} = \underline{\underline{A}}^{-1}(\underline{x}) \cdot \underline{b}$ is written in finite differences by using the fourth order Runge-Kutta method to get the discrete vector $\underline{x}$. Therefore, from the perturbed 2-D model, we calculate the temperature field from the perturbed energy balance written in finite differences. The resulting tri-diagonal matrix for the unknown values of temperatures at the grid points requires the discrete temperature values at the free surface evaluated from the perturbed version of Eq. (10). In addition, the stress fields are obtained from the PTTM written in finite differences (an explicit-implicit scheme is used) for each axial position Z and any ζ to obtain their average values. Therefore, the structure of the numerical algorithm consists in solving at each axial step the temperature and stress fields to calculate the non-linear averages and internal heat transfer coefficient required in the perturbed average model. These calculations are carried out iteratively at each axial step, where convergence criteria must be satisfied for the resulting average temperature and stress fields from the perturbed 2-D and average models, thus indicating consistency of these models with the averages process. The iterative process also requires two additional convergence criteria associated with the determination of the length L, where the glass temperature is reached and the filament starts to move at the take-up velocity.

4 RESULTS AND DISCUSSION

Figure 1 shows curves of the rheometric and process elongational viscosities (see Eqs. (13) to (15)) for the PET under study. One observes in this figure that the spinning curve is obtained for different values of $f = \partial v_z / \partial Z$ at $Z = 0$, when v_L = 3000 m/min, *DR*=165, v_s = 0.303 m/s, $r_s = 2\,r_c$ and α = 0.85. Thus by increasing *f*, the values of the process elongational viscosity at the spinning onset (*Z*=0) decrease, crossing the rheometric elongational viscosity until a minimum value is obtained for around $f \approx 19$. In this figure, one can also read at the abscissa coordinate the process elongational rate for *Z*=0 at each value f, which becomes higher as f increases. Afterward, at a fixed value of f, as the process elongational rate is higher for *Z*>0, the corresponding process elongational viscosity follows a similar shape as that of the rheometric one. From the physical point of view, it is clear that both viscosities should be monotonic increasing functions of the process and rheometric elongational rates, respectively, at the starting zone of the onset of the spinning flow (a condition of the initial stretching flow). This physical aspect places a clear mathematical constraint that allows the algorithm to determine the unknown derivative $f = \partial v_z / \partial Z$ at $Z = 0$, and hence to show that the stretching spinning flow does not necessarily start from the maximum swelling with $f = 0$. Thus, for the particular case illustrated in this figure, f =19 is appropriate as long as the PTTM with a retarded elastic response applies (α = 0.85).

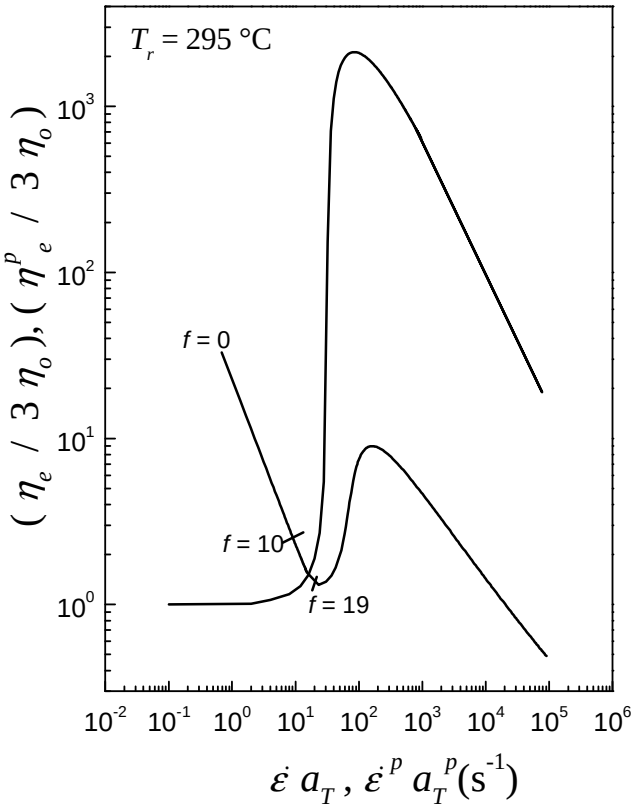

Figure 1: Rheometric and process elongational viscosities as a function of rheometric and process elongational rates for PET. The variation of derivative f at Z = 0 for α = 0.85 is illustrated on the process elongational viscosity curve through small cutting lines.

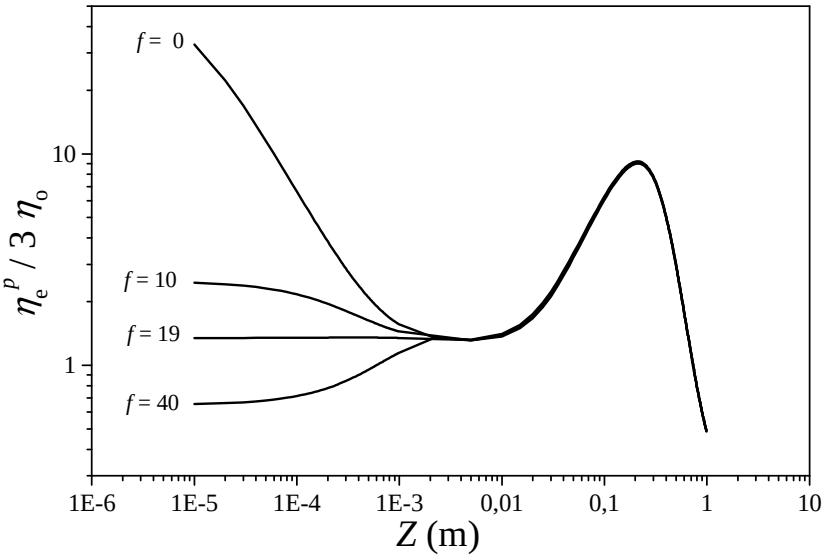

Figure 2: Process elongational viscosity as a function of axial distance. Variation of derivative f at $Z = 0$ for $\alpha = 0.85$.

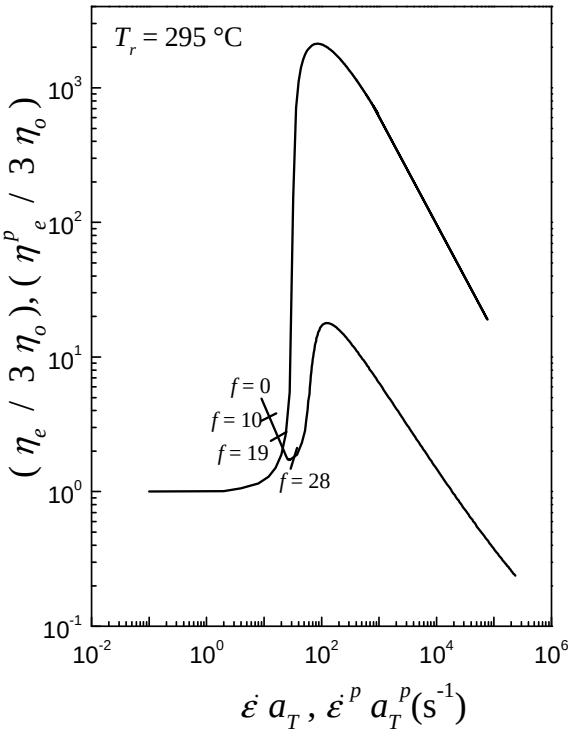

Figure 3: Rheometric and process elongational viscosities as a function of rheometric and process elongational rates. The variation of derivative f at $Z = 0$ for $\alpha = 0.99$ is illustrated on the process elongational viscosity curve through small cutting lines.

Figure 2 shows clearly that different values of f at $Z = 0$ affect the spinning solution only along a small distance of the order of 10^{-3} m. The solution expected for $f = 19$ is also

illustrated here. This figure also shows numerical results for $f > 19$ to observe an unexpected physical result again. Thus the process elongational viscosity from the physical point of view is a constant function of the axial coordinate at the onset of the spinning process.

Finally, Figures 3 and 4 show the effect of f at $Z = 0$ on the process elongational viscosity, when one considers the PET with an almost instantaneous elastic response ($\alpha \to 1$). Thus retardation effects are asymptotically small. These figures show that the zone where solutions are sensitive to variations of f is substantially smaller than that of Figures 1 and 2; thus in Figure 4 this zone is of the order of 9 10^{-5} m. For this asymptotic material response the appropriate physical value is $f \approx 28$.

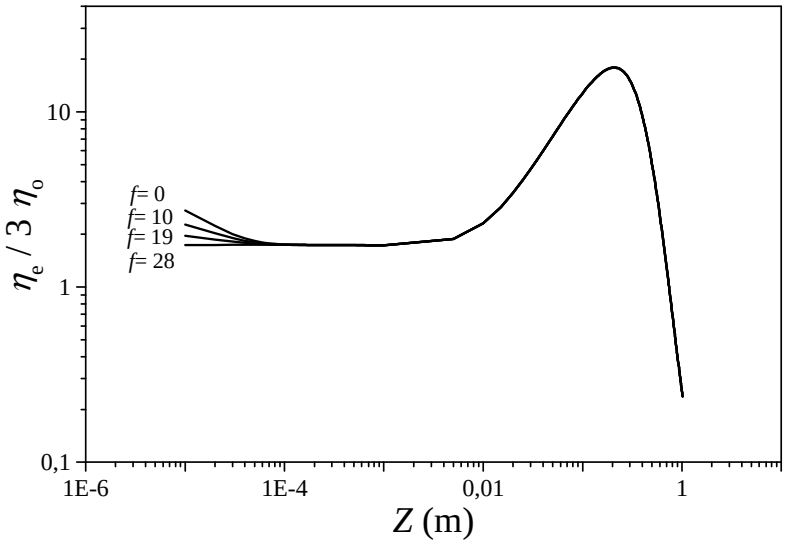

Figure 4: Process elongational viscosity as a function of axial distance. Variation of parameter f at $Z = 0$ for $\alpha = 0.99$.

5 CONCLUSIONS

Numerical results indicate that the initial slope of the axial velocity is appropriately defined and has a unique value as long as the process elongational viscosity satisfies the constraint of being a monotonic increasing function of the process elongational rate at the onset of the spinning flow. Also non unique solutions generated by the ill-posed problem, associated with the spinning initial conditions, are confined along a negligible zone at the beginning of the spinneret, which becomes smaller when the melt approaches the instantaneous elastic response.

Acknowledgments

Authors wish to thank the financial aid received from Universidad Nacional del Litoral, Santa Fe, Argentina (CAI+D 2006) and CONICET (PIP 5728).

REFERENCES

Deiber, J. A. and Schowalter, W. R. Flow through Tubes with Sinusoidal Axial Variations in Diameter. *AIChE J.*, 25: 638-645, 1979.

Denn, M. M., Petrie C. J. S. and Avenas P. Mechanics of Steady Spinning of a Viscoelastic Liquid. *AIChE J.*, 21: 791-799, 1975.

Denn, M. M. *Computational Analysis of Polymer Processing*. Pearson, J. R. A., Richardson, S. M. Eds.; Applied Science Publishers. New York, 1983.

Denn, M. M. Continuous Drawing of Liquids to form Fibers. *Ann. Rev. Fluid Mech*., 12: 365-387, 1980.

Denn, M. M. Correlations for Transport Coefficients in Textile Fiber Spinning. *Ind. Eng. Chem. Res.*, 35: 2842-2843, 1996.

Gagon, D. K. and Denn, M. M. Computer Simulation of Steady Polymer Melt Spinning. *Polym. Eng. Sci*., 21: 844-853, 1981.

George, H. H. Model of Steady-State Melt Spinning at Intermediate Take-Up Speeds. *Polym. Eng. Sci*., 22: 292-299, 1982.

Gregory, D. R. and Watson, M. T. Steady State Properties of Poly(Ethylene Terephthalate) Melts. *J. Polym. Sci*., 30: 399-406, 1970.

Henson, G. M., Cao, D., Bechtel, S. E., and Forest, M. G. A. Thin-Filament Melt Spinning Model with Radial Resolution of Temperature and Stress. *J. Rheol.*, 42: 329-360, 1998.

Keunings, R., Crochet, M. J. and Denn, M. M. Profile Development in Continuous Drawing of Viscoelastic Liquids. *Ind. Eng. Chem. Fundam.*, 22: 347-355**,** 1983.

Ottone, M. L. and Deiber, J. A. Modeling the Melt Spinning of Polyethylene Terephthalate. *J. Elast. Plast*., 32**:** 119-139, 2000.

Ottone, M. L and Deiber, J. A. A Numerical Method for the Viscoelastic Melt Spinning Model with Radial Resolutions of Temperature and Stress Field. *Ind. Eng. Chem. Res.*, 41:6345-6353, 2002.